

Catalysis of the Addition of Benzenethiol to 2-Cyclohexen-1-ones by Uranyl–Salophen Complexes: A Catalytic Metallocleft with High Substrate Specificity

Valeria van Axel Castelli,^[a] Antonella Dalla Cort,^[a] Luigi Mandolini,^{*,[a]} David N. Reinhoudt,^{*,[b]} and Luca Schiaffino^[a]

Abstract: The base induced addition of benzenethiol to 2-cyclohexen-1-one and its 4,4-, 5,5- and 6,6-dimethyl derivatives is catalysed by a salophen–uranyl based metallocleft **2** in chloroform solution with high turnover efficiency and low product inhibition. Analysis of rate data coupled with equilibrium measurements for complexation of the catalyst with the enone reactants and addition products shows that the catalytic mechanism involves the three main steps typical of single-substrate enzymatic processes, namely substrate binding and recognition, transformation of the bound substrate, and release of the reaction product. Unlike the reference salophen–uranyl **1**, catalyst **2** is endowed with a structured binding site responsible for a high degree of substrate specificity among the investigated enones, due to recognition of their shape and size.

Keywords: enzyme mimetics • kinetics • Michael additions • substrate specificity • supramolecular metallocatalysts

Introduction

The design and synthesis of abiotic catalysts that mimic the fundamental features of enzymatic catalysis is an important area of current research in supramolecular chemistry.^[1] Among the various features which are worth mimicking in artificial systems, substrate specificity occupies a prominent role. Specific binding to a substrate requires that the enzyme binding site is complementary in structure to the structure of the substrate.^[2] Hence a highly structured binding site is a prerequisite for a high degree of substrate specificity in a synthetic catalyst.

We have recently reported^[3] that the robust salophen–uranyl complexes **1** and **2** catalyse the addition of benzenethiol to 2-cyclopenten-1-one [Equation (1)] with high turnover efficiency and low product inhibition. The schematic picture of the transition state given in Figure 1 illustrates the

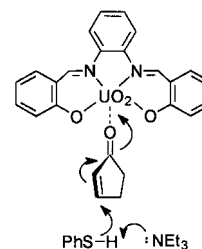
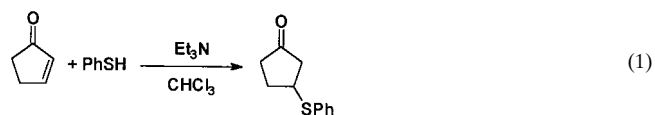


Figure 1. Schematic picture of the transition state of the rate-determining step, showing concerted Brønsted base activation of the thiol nucleophile and Lewis acid activation of the enone electrophile.

combination of two complementary catalytic actions. The Brønsted base activates the thiol nucleophile, whereas the metal centre provides the enone electrophile with Lewis acid activation through coordination of the carbonyl oxygen to the fifth equatorial coordination site.^[4]

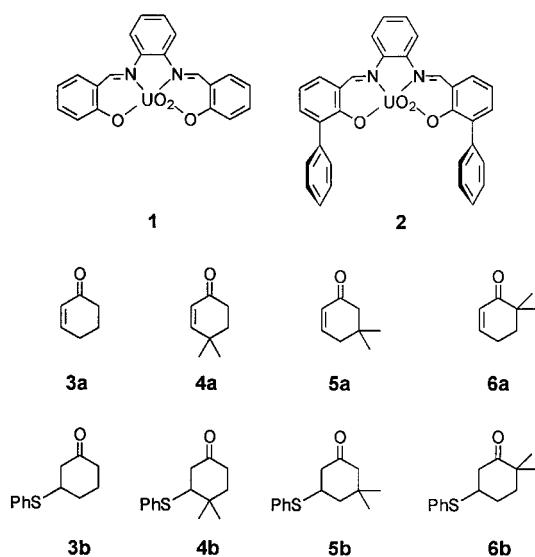


The fifth equatorial site of the uranyl unit in complex **2** is available for coordination to a guest molecule only if the two phenyl groups are parallel to one another and form the walls of a narrow cleft.^[5] Thus, the reaction of a bound substrate is forced to take place in the neighbourhood of the cleft walls. Consequently this reaction should be very sensitive to steric effects in general and, more specifically, to the shape of the substrate.

[a] Prof. L. Mandolini, Dr. V. van Axel Castelli, Dr. A. Dalla Cort, Dr. L. Schiaffino
Dipartimento di Chimica and Centro CNR Meccanismi di Reazione
Università La Sapienza
Box 34, Roma 62, 00185 Roma (Italy)
Fax: (+39)06490421
E-mail: lmandolini@uniroma1.it

[b] Prof. D. N. Reinhoudt
University of Twente, Faculty of Chemical Technology
Laboratories of Supramolecular Chemistry and Technology
and MESA Research Institute
P.O. Box 217, 7500 AE Enschede (The Netherlands)
Fax: (+31) 53-4894645
E-mail: d.n.reinhoudt@ct.utwente.nl

With this idea in mind, and in view of the importance of Michael-type addition of thiols to activated olefins both in biochemical processes^[6] and in synthesis,^[7] we have carried out a thorough kinetic study of the catalytic properties of metalocleft **2** in the addition of benzenethiol to 2-cyclohexen-1-one (**3a**) and its dimethyl derivatives **4a–6a** in the presence of Et₃N in chloroform at 25 °C. Enones **4a–6a** form a series of compounds with very similar electronic properties but quite different geometrical features. Complex **1** has been investigated as a reference catalyst to probe the Lewis acid properties of the metal centre. Competition experiments have been carried out on selected pairs of substrates to illustrate the high degree of substrate specificity experienced by catalyst **2**.



Results and Discussion

Complexation equilibria: Since complexes with definite stability of the enone reactants and ketone products with the metal catalyst are involved in the catalytic processes, preliminary to the kinetic investigation, we have determined the relevant binding constants. A standard UV/Vis titration technique was used in most cases. Since mixtures of metal complex **2** and enone **3a** turned out to be highly unstable upon irradiation, as shown by irreproducible and time dependent absorbance readings, this binding constant was determined by a ¹H-NMR titration technique. When applied to the corresponding complex formed by **2** and **4a**, the two techniques afforded K_E values in good agreement with each other, as shown in Table 1 where binding data are collected. Typical titration curves are shown in Figures 2 and 3.

Structural information on the geometry of the complexes formed with **2** is provided by the ¹H-NMR data. The upfield shifts observed upon addition of **2** for the hydrogens on C₅ and C₆ of **4a** (Figure 3) clearly suggest that these hydrogens are exposed to the shielding cones of the phenyl groups of **2**. Variations of the chemical shifts of the hydrogens on the double bond are also upfield, but much smaller in magnitude,

Table 1. Equilibrium constants (M⁻¹)^[a] for association of metal complexes **1** and **2** with enones **3a–6a** (K_E) and the corresponding reaction products **3b–6b** (K_P) in chloroform at 25.0 °C.

guest	1		2	
	K_E	K_P	K_E	K_P
3 (a or b)	7.6 ± 0.6	< 2	900 ± 200 ^[b]	104 ± 16
4 (a or b)	17 ± 2	< 2	820 ± 150 ^[c]	244 ± 16
5 (a or b)	4 ± 1	< 2	133 ± 16	70 ± 7
6 (a or b)	ca. 3	< 2	6.4 ± 1.4	< 2

[a] From UV/Vis titrations, when otherwise stated. Error limits were calculated as $\pm 2\sigma$. [b] From ¹H-NMR titration. [c] $K_E = 760 \pm 100$ from ¹H-NMR titration.

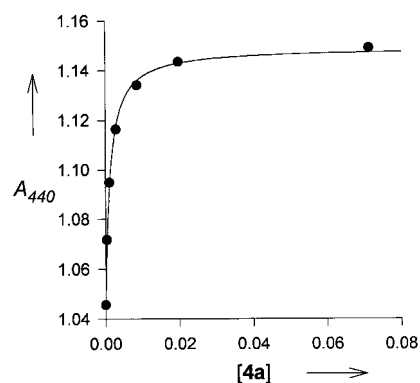


Figure 2. UV/Vis titration of **2** with **4a** ($\lambda = 440$ nm). The points are experimental and the curve is calculated from a 1:1 binding isotherm equation with $K_E = 820$ M⁻¹ and $A_{\infty} = 1.149$.

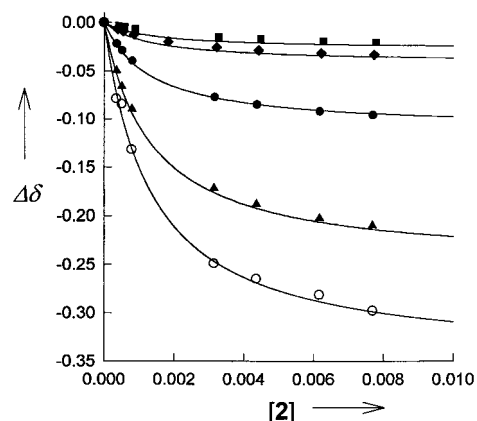


Figure 3. ¹H-NMR titration of **4a** with **2**. Data points refer to chemical shift variations of the signals of the protons on C₂ (■), C₃ (◆), CH₃ (●), C₆ (▲), C₅ (○). The curves are calculated with $K_E = 760$ M⁻¹.

probably because a deshielding effect due to electron withdrawal from the complexed carbonyl group is superimposed on the shielding effect of the aromatic cleft walls.^[5] The modest upfield shift of the methyl hydrogens suggests a marginal location of the *gem*-dimethyl group in the cleft. Similar results were obtained for the complex of **2** with **3a**. The picture that emerges from the above observations is clearly one in which the enone guest is bound via its carbonyl group to the fifth coordination site of the uranium, and is located in the inside of the cleft. Stabilising interactions are established between the hosted substrates and the cleft walls, as shown by the finding that host **2** is a much stronger binder than its parent compound **1** of all of the investigated

substrates. This indicates that the internuclear distances between the cleft walls and the hosted substrates are for the most part in the attractive regions of van der Waals interactions. Host **2** is much more sensitive to the steric requirements of the guest than its parent compound **1**. Both K_E and K_P values with **2** markedly decrease in the order $4 > 5 > 6$; this shows that the steric hindrance in the complexation of the bulky *gem*-dimethyl group increases when its distance from the carbonyl group decreases. The α,β -unsaturated ketones are stronger Lewis bases than the saturated ketones caused by the strong conjugation of the double bond with the carbonyl group. This finding has important consequences on the catalytic properties of **1** and **2**, in that the adverse influences of product inhibition are significantly reduced.

Other effects of structure on complex stability are less easily understood. For example, a *gem*-dimethyl group in position 4 increases the stability of the complex (K_E) of **1** with **4a** compared with **3a**, and that of **2** with **4b** compared with **3b**, but complexes of **2** with **4a** and **3a** show the same stability within experimental errors. It seems likely that these effects are due to a subtle interplay of electronic and steric effects, with the possible involvement of solvation effects.

Kinetics: Rate measurements were carried out by $^1\text{H-NMR}$ spectroscopy both in the absence and presence of metal catalyst. Typical time-concentration data are plotted in Figure 4. In all cases the disappearance of the enone reactant was

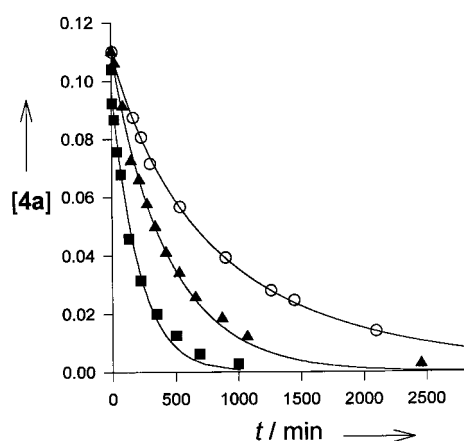
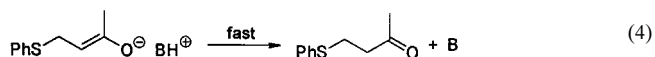
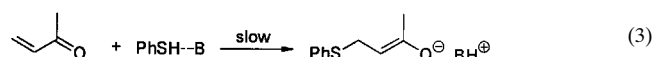


Figure 4. $^1\text{H-NMR}$ time-concentration data for the addition of 0.21M benzenethiol to 0.11M enone **4a** in the presence of 4.9mM Et_3N : (○) Et_3N alone, (■) Et_3N plus 1.0mM **1**, (▲) Et_3N plus 1.0mM **2**. The curves are calculated from the second-order rate equation for the reaction carried out with Et_3N alone, and from Equation (12) in the presence of metal catalyst.

complete and the formation of the equivalent amount of addition product was observed. In no case extra peaks due to reaction intermediates and/or side products were observed. Since the amount of catalyst is 1 mol% of the initial enone concentration, nearly one hundred turnovers are actually observed when contributions from the uncatalysed reaction are very small.

The generally accepted mechanism^[8] of the Michael-type addition of thiols to activated olefins in the presence of a tertiary base B in solvents of low polarity involves rate-limiting addition of the thiolate of a rapidly formed 1:1

complex of thiol and base, to give a BH^+ -enolate ion pair intermediate, followed by fast proton transfer from BH^+ to the enolate [Equations (2)–(4)]. It is uncertain whether the

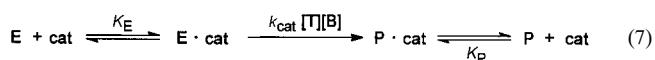


thiol-base complex has the structure of a hydrogen-bonded pair ($\text{Ph-SH}\cdots\text{B}$) or of an ion pair ($\text{PhS}^- \text{HB}^+$).^[8] In any case, because of the insignificant formation of the thiol-base adduct, the above mechanism leads to clean third-order kinetics [Equation (5)], first-order in the enone E, thiol T, and base B. Since the concentration of the base catalyst is constant in a given run, a second-order time dependence is actually predicted [Equation (6)] with $k_{\text{obs}} = k_o[\text{B}]$. Consistently, all of the runs carried out in the absence of metal catalyst showed a close adherence to second-order kinetics. A typical time-concentration profile is shown in Figure 4.

$$v_o = k_o[\text{E}][\text{T}][\text{B}] \quad (5)$$

$$v_o = k_{\text{obs}}[\text{E}][\text{T}] \quad (6)$$

In the presence of metal catalyst^[3] the reaction is conveniently described according to the Equation (7) as a third-order reaction between T, B, and an enone-catalyst complex ($\text{E}\cdot\text{cat}$) as shown in Equation (8). When the fraction of



$$v_{\text{cat}} = k_{\text{cat}}[\text{E}\cdot\text{cat}][\text{T}][\text{B}] \quad (8)$$

catalyst sequestered by the enone reactant and by the reaction product P is taken into account, Equation (8) is easily transformed into Equation (9), that holds whenever $[\text{cat}]_{\text{tot}} \ll [\text{E}]$. Integration of Equation (9) by standard methods leads to Equation (10) which applies when the initial concentrations of the reactants are not equal and when the rate of the uncatalysed reaction is negligible compared with the catalysed one.

$$v_{\text{cat}} = \frac{k_{\text{cat}} K_E [\text{E}][\text{T}][\text{B}][\text{cat}]_{\text{tot}}}{1 + K_E[\text{E}] + K_P[\text{P}]} \quad (9)$$

$$\frac{K_P [\text{E}]_o + 1}{k_{\text{cat}} K_E [\text{B}][\text{cat}]_{\text{tot}}([\text{T}]_o - [\text{E}]_o)} \ln \frac{[\text{E}]_o}{[\text{E}]} + \left(\frac{(K_E - K_P)([\text{T}]_o - [\text{E}]_o) - K_P[\text{E}]_o - 1}{k_{\text{cat}} K_E [\text{B}][\text{cat}]_{\text{tot}}([\text{T}]_o - [\text{E}]_o)} \right) \ln \frac{[\text{T}]_o}{[\text{T}]} = t \quad (10)$$

When this is not the case, the overall reaction rate is given by the sum of two contributions [Equation (11)]. Substitution of Equations (5) and (9) into Equation (11), followed by integration, leads to Equation (12), that again applies to the case of different reactant concentrations, and where the quantities a and b are defined in Equations (13) and (14), respectively.

$$v_{\text{tot}} = v_o + v_{\text{cat}} \quad (11)$$

$$\frac{K_P [E]_o + 1}{a ([T]_o - [E]_o)} \ln \frac{[E]_o}{[E]} + \left(\frac{K_E - K_P}{a - b} - \frac{K_P [E]_o + 1}{(a - b) ([T]_o - [E]_o)} \right) \ln \frac{[T]_o}{[T]} + \frac{(K_E - K_P) k_{\text{cat}} K_E [B] [\text{cat}]_{\text{tot}}}{a (a - b)} \ln \left(1 - \frac{(K_E - K_P) k_o ([E]_o - [E])}{k_o + k_{\text{cat}} K_E [\text{cat}]_{\text{tot}} + k_o K_E [E]_o} \right) = t \quad (12)$$

$$a = k_o [B] (K_P [E]_o + 1) + k_{\text{cat}} K_E [B] [\text{cat}]_{\text{tot}} \quad (13)$$

$$b = k_o [B] ([T]_o - [E]_o) (K_E - K_P) \quad (14)$$

Equations (10) and (12) are rather complicated expressions. However, since K_E and K_P are independently known, and since the composition of the mixture at any time is known from $^1\text{H-NMR}$ data, the left-hand terms contain k_{cat} as the only unknown quantity. For each catalytic experiment a k_{cat} value was selected using a computer programme such that the left side of Equation (10) or, whenever appropriate, Equation (12) plots against time as a straight line with unit slope and zero intercept. An example of such a plot is shown in Figure 5. The time-concentration profiles recalculated with the best fit k_{cat} values reproduce to a good precision the experimental data (Figure 4).

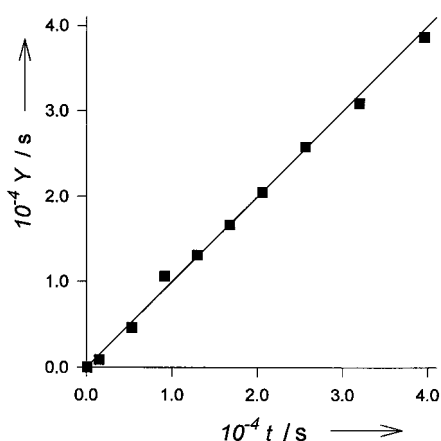


Figure 5. Plot of the left side of Equation (12) Y against time for the addition of benzenethiol to **4a** catalysed by Et_3N plus **2**, showing good adherence of data points to the straight line having slope 1 and intercept 0.

Kinetic data are collected in Table 2. The k_{cat} is a third-order rate constant that refers to the reaction of the catalyst–substrate complex (high substrate concentration, saturating conditions), whereas $k_{\text{cat}}K_E$ is a fourth-order rate constant that refers to the reaction of the free substrate and free catalyst (low substrate concentration, subsaturating conditions). Discrimination between two or more competing substrates is determined by the ratios of $k_{\text{cat}}K_E$ at all concentrations of substrates.

Table 2 shows that in the reference reaction (k_o) reactivity decreases in the order **3a** > **6a** > **5a** > **4a**, which provides clear evidence that the reaction is sensitive to the steric bulk of the *gem*-dimethyl group, as well as to its distance from the site of nucleophilic attack. Both k_{cat} and $k_{\text{cat}}K_E$ values obtained in the presence of catalyst **1** decrease in the same order as the reference reaction, but span significantly wider

Table 2. Kinetics data^[a] for the Et_3N assisted addition of benzenethiol to enones **3a–6a** in CDCl_3 at 25.0°C in the absence and presence of salophen–uranyl complexes **1** and **2**. The reactions of **4a** were taken as reference for the calculation of relative values given in parentheses.

	Et_3N		$\text{Et}_3\text{N}+\mathbf{1}$		$\text{Et}_3\text{N}+\mathbf{2}$		
	k_o	k_{cat}	k_{cat}/k_o	$k_{\text{cat}}K_E$	k_{cat}	k_{cat}/k_o	$k_{\text{cat}}K_E$
3a	0.66 (27.5)	1550 (155)	2300 (69)	11 800	710 (394)	1100 (430)	640 000
4a	0.024 (1.0)	10 (1.0)	420 (1.0)	170	1.8 (1.0)	75 (1.0)	1500
5a	0.080 (3.3)	325 (32.5)	4100 (7.6)	1300	98 (54)	1200 (8.7)	13 000
6a	0.14 (5.8)	480 (48)	3400 (8.2)	1400	2.6 (1.4)	19 (0.011)	17

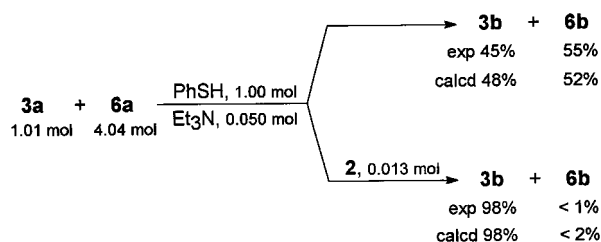
[a] The various quantities are defined in Equations (5) and (8). Rate constants k_o and k_{cat} are given in $(\text{M}^{-2}\text{s}^{-1})$. Estimated uncertainties are in the order of ± 4 –10%.

ranges. This indicates that the catalysed reaction exhibits an increased sensitivity to steric effects. Incidentally, we like to emphasise that the reaction catalysed by **1** provides a violation of the so-called reactivity–selectivity principle, in that the higher substrate selectivity is displayed by the faster reaction.^[9]

Even wider ranges are spanned by the k_{cat} and $k_{\text{cat}}K_E$ values obtained in the presence of catalyst **2**. Here the reactivity order is significantly different from the “natural” order exhibited by the reference reaction. The reactivity of **6a** is extremely low, particularly with reference to $k_{\text{cat}}K_E$, whose magnitude is the result of unfavourable combination of a very low affinity toward the catalyst, and a very low reactivity of the catalyst–substrate complex.

From the data above it is apparent that substrate **6a** ranks next in reactivity to the most reactive **3a** both in the reference reaction and in the reaction catalysed by **1**. However it is definitely the substrate with the lowest $k_{\text{cat}}K_E$ value in the presence of catalyst **2**. Since discrimination between two competing substrates is determined by the relative magnitude of $k_{\text{cat}}K_E$, a number of competition experiments were designed based on the data in Table 2 in order to illustrate substrate specificity as a distinctive feature of catalyst **2** due to its metallocleft structure.

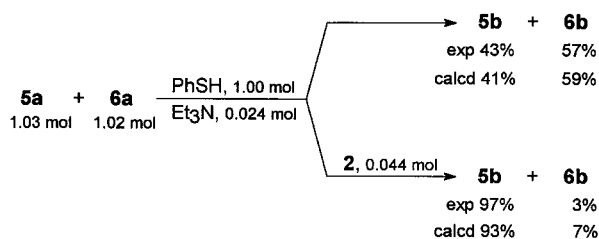
In one experiment, a mixture of 0.099 M **3a** and 0.395 M **6a** was combined with 0.098 M benzenethiol in the presence of 4.9 mM Et_3N . As shown in Scheme 1 we found a nearly even distribution of benzenethiol among reactants, in good agreement with calculations based on the kinetics. However, on addition of 1.3 mM **2** the same reaction mixture gave, as



Scheme 1. Competition experiment between **3a** and **6a** in the absence and presence of metallocleft **2**.

predicted, adduct **3b** as the sole detectable product in virtually quantitative yield. Clearly, the reactivity difference between enones **3a** and **6a**, which amounts to a factor 4 in favour of the former, is magnified to such an extent by metallocleft **2**, that adduct **3b** is the sole product. This is a remarkable result if one considers that the **6a:3a** mole ratio is 4:1 at time zero, but increases dramatically toward the end of reaction.^[10]

In another experiment a mixture of 0.101 M **5a** and 0.100 M **6a** was reacted with 0.098 M benzenethiol in the presence of 2.3 mM Et₃N and in the presence of 2.3 mM Et₃N plus 4.3 mM **2** (Scheme 2). Again a profound change in the final composition is caused by the presence of **2**. A rather unselective reaction is transformed into a very selective reaction, where benzenethiol is directed almost exclusively toward the formation of adduct **5b**. Unlike the previous example, here the good substrate for the catalyst is the one with the lower intrinsic reactivity. Since **5a** and **6a** are isomeric substrates, the selection process is clearly based on recognition of their different shapes.



Scheme 2. Competition experiment between **5a** and **6a** in the absence and presence of metallocleft **2**.

Conclusion

In conclusion, the salophen–uranyl metallocleft **2** provides a remarkable example of a supramolecular catalyst. Fairly high reaction rates, high turnover efficiency and low product inhibition are accompanied by a high degree of substrate specificity which is lacking in the reaction solely catalysed by Et₃N, or by a combination of Et₃N and **1**. Current work is devoted at shaping the catalyst binding site in such a way as to achieve enantioselective catalytic process.

Experimental Section

Instruments and methods: ¹H- and ¹³C-NMR spectra were recorded in CDCl₃ with either a Bruker AC200 or a Bruker AC300 spectrometer. UV/Vis spectra were recorded with a Perkin–Elmer Lambda 18 spectrophotometer. Nonlinear least-squares calculations were carried out using the programme SigmaPlot for Windows, 1.02 (Jandel Scientific). Numerical integrations of experimental data were carried out using the programme Scientist for Windows, 2.0 (MicroMath Inc.).

Materials: Benzenethiol (Fluka) and 2-cyclohexen-1-one (**3a**) (Aldrich) were distilled under reduced pressure before use. Triethylamine (Aldrich) was distilled over sodium. Spectrophotometric grade chloroform (Aldrich) and CDCl₃ (Merck) were dried over 4 Å molecular sieves for at least 24 h prior to use. 4,4-Dimethyl-2-cyclohexen-1-one (**4a**) (Aldrich) was used as received. Salophen–uranyl complexes **1** and **2** were available from a previous work.^[3] 5,5-Dimethyl-2-cyclohexen-1-one (**5a**),^[11] 6,6-dimethyl-2-

cyclohexen-1-one (**6a**),^[12] 3-(phenylthio)cyclohexanone (**3b**),^[13] and 4,4-dimethyl-3-(phenylthio)cyclohexanone (**4b**),^[14] m.p. 61–62 °C, lit.: 62 °C^[14] were prepared according to literature procedures. These compounds showed spectral data consistent with expected structures. 5,5-Dimethyl-3-(phenylthio)cyclohexanone (**5b**) and 6,6-dimethyl-3-(phenylthio)cyclohexanone (**6b**) were prepared according to a general procedure.^[15]

5,5-Dimethyl-3-(phenylthio)cyclohexanone (5b): This compound was obtained as an oil after flash chromatography on silica gel with petroleum ether/diethyl ether 6:1 (61 %). ¹H NMR (300 MHz, CDCl₃, 25.0 °C, TMS): δ = 7.26–7.42 (m, 5H), 3.36–3.47 (m, 1H), 2.59–2.66 (m, 1H), 2.06–2.29 (m, 3H), 1.91–1.92 (m, 1H), 1.60–1.69 (m, 1H), 1.07 (s, 3H), 0.89 (s, 3H); ¹³C NMR: 25.61, 31.76, 35.22, 42.40, 45.05, 47.65, 54.06, 127.80, 129.09, 132.89, 133.12, 208.87; elemental analysis for C₁₄H₁₈SO (234.1): calcd C 71.75, H 7.74; found: C 71.6, H 7.7.

6,6-Dimethyl-3-(phenylthio)cyclohexanone (6b): This compound was obtained as an oil after flash chromatography on silica gel with 3 % ethyl acetate in petroleum ether (61 %). ¹H NMR (300 MHz, CDCl₃, 25.0 °C, TMS): δ = 7.27–7.45 (m, 5H), 3.31–3.46 (m, 1H), 2.48–2.69 (m, 2H), 1.78–2.09 (m, 3H), 1.54–1.64 (m, 1H), 1.13 (s, 3H), 1.06 (s, 3H); ¹³C NMR: 24.82, 24.96, 27.82, 38.29, 44.13, 44.40, 46.64, 127.63, 129.00, 133.00, 133.15, 212.81; elemental analysis for C₁₄H₁₈SO (234.1): calcd C 71.75, H 7.74; found: C 72.0, H 7.8.

Equilibrium measurements: Solutions were prepared and handled under argon to minimise contamination by atmospheric oxygen and water. UV/Vis titrations were carried out at 25.0 °C in CHCl₃ by adding increasing amounts of the ketone to a 0.1 mM solution of the salophen–uranyl complex and following variations of absorbance at 430 nm with **1** and 440 nm with **2**. ¹H-NMR titrations were carried out at 25.0 °C in CDCl₃ by adding increasing amounts of the salophen–uranyl complex to a 1 mM solution of the ketone and by following variations of the chemical shift of ketone signals. Titrations data were fitted to a standard binding isotherm for 1:1 complexation.

Rate measurements: NMR tubes were dried in an oven at 130 °C for at least 24 h and then stored in a desiccator. All sample manipulations were carried out under an argon atmosphere. Calculated amounts of triphenylmethane (internal standard) and of all of the reactants except Et₃N were introduced into a NMR tube and a spectrum (either at 200 or 300 MHz, T = 25.0 °C) was recorded at time zero. Then a given amount of Et₃N was added, and spectra were recorded at selected time intervals. The intensity of the signal of the α proton of the double bond (δ ca. 6) of the enone was compared with that of the signal of the internal standard. Time-concentration data obtained in the absence of metal catalyst were fitted to the standard second-order equation, and the obtained second-order rate constant was translated into the third-order rate constant k_o. Data obtained in the presence of the metal catalyst were fitted to Equation (10) or (12). Because of the mathematical form of these equations, the enone concentration was taken as the independent variable in the curve-fitting procedure.

Competition experiments: Reaction mixtures were prepared according to the same procedure used for rate measurements. After the addition of Et₃N, ¹H-NMR spectra were recorded as a function of time until no further changes were observed in repeated spectra and all benzenethiol had been consumed. Final concentrations were measured by comparing initial and final integrated intensities of the signals of the α proton of the two enones with the signal of the internal standard.

Acknowledgement

Thanks are due to MURST for financial support of this work in the frame of a research project on “Supramolecular Devices”.

- [1] a) R. Breslow, *Acc. Chem. Res.* **1995**, *28*, 146–153; b) J.-M. Lehn, *Supramolecular Chemistry*, VCH, Weinheim, **1995**, Ch. 5; c) A. J. Kirby, *Angew. Chem.* **1996**, *108*, 770–790; *Angew. Chem. Int. Ed. Engl.* **1996**, *35*, 707–724; d) Y. Murakami, J. Kikuchi, Y. Hisaeda, O. Hayashida, *Chem. Rev.* **1996**, *96*, 721–758; e) M. C. Feiters in *Comprehensive Supramolecular Chemistry*, Vol. 10 (Eds.: J. L. Atwood, J. E. D. Davies, D. D. MacNicol, F. Vögtle), Pergamon, Oxford,

- 1996, pp. 267–514; f) J. K. M. Sanders, *Chem. Eur. J.* **1998**, *4*, 1378–1383.
- [2] A. Fersht, *Enzyme Structure and Mechanism*, 2nd ed., Freeman, New York, **1985**, pp. 347–368.
- [3] V. van Axel Castelli, A. Dalla Cort, L. Mandolini, D. N. Reinhoudt, *J. Am. Chem. Soc.* **1998**, *120*, 12688–12689.
- [4] V. van Axel Castelli, R. Cacciapaglia, G. Chiosis, F. C. J. M. van Veggel, L. Mandolini, D. N. Reinhoudt, *Inorg. Chim. Acta* **1996**, *246*, 181–193.
- [5] A. R. van Doorn, M. Bos, S. Harkema, J. van Eerden, W. Verboom, D. N. Reinhoudt, *J. Org. Chem.* **1991**, *56*, 2371–2380.
- [6] a) A. L. Fluharty in *The Chemistry of the Thiol Group, Part 2* (Ed.: S. Patai), Wiley, New York, **1974**, pp. 589–668; b) B. E. Thomas IV, P. A. Kollman, *J. Org. Chem.* **1995**, *60*, 8375–8381, and references therein.
- [7] a) H. Wynberg, in *Topics in Stereochemistry, Vol. 16* (Eds.: E. L. Eliel, S. H. Wilen, N. L. Allinger), Wiley, New York, **1986**, pp. 87–129; b) E. Emori, T. Arai, H. Sasai, M. Shibasaki, *J. Am. Chem. Soc.* **1998**, *120*, 4043–4044, and references therein.
- [8] a) B. Dmuchovsky, B. D. Vineyard, F. B. Zienty, *J. Am. Chem. Soc.* **1964**, *86*, 2874–2877; b) H. Hiemstra, H. Wynberg, *J. Am. Chem. Soc.* **1981**, *103*, 417–430.
- [9] C. D. Johnson, *Tetrahedron* **1980**, *36*, 3641–3680.
- [10] From the data in Table 2 it is easily calculated that **2** picks out and delivers to benzenethiol one molecule of **3a** mixed with 99 molecules of **6a** with a probability of 99.7%. The small (ca. 2%) calculated yield of **6b** in the final reaction mixture is almost exclusively due to the competing background reaction.
- [11] R. L. Frank, H. K. Hall, Jr., *J. Am. Chem. Soc.* **1950**, *72*, 1645–1648.
- [12] C. Freppel, M. A. Poirer, J. C. Richer, Y. Maroni, G. Manuel, *Can. J. Chem.* **1974**, *52*, 4133–4138.
- [13] P. Chamberlain, G. H. Whitham, *J. Chem. Soc. Perkin Trans. II* **1972**, 130–135.
- [14] L. Angiolini, D. Caretti, C. Carlini, E. Salatelli, G. Sciacca, *Gazz. Chim. Ital.* **1996**, *126*, 69–74.
- [15] P. Bakuzis, M. L. F. Bakuzis, *J. Org. Chem.* **1981**, *46*, 235–239.

Received: May 17, 1999 [F1790]